

ARTICLE

Electrochemical Determination of Omeprazole at Molybdenum Disulfide Modified Glassy Carbon Electrodes**Mohammad F. Khanfar^{a*}, Eyad S. M. Abu-Nameh^{b*}, Salsabeel AlSawa'eer^b, Munib M. Saket^a, Ahlam Al Kselat^a, Amira Zidan^a and Sameer A. Hasan^c**^aDepartment of Pharmaceutical and Chemical Engineering, School of Applied Medical Sciences, German Jordanian University, P.O.Box 35247 Amman 11180 Jordan.^bDepartment of Chemistry, Faculty of Science, Al-Balqa Applied University, Al-Salt 19117, Jordan.^cBiomedical Engineering Department, School of Applied Medical Sciences, German Jordanian University, P.O.Box 35247 Amman 11180 Jordan.Received: 3rd Oct. 2022;Accepted: 27th April 2023

Abstract: Molybdenum disulfide, MoS₂, is commonly used as a substrate in supercapacitors and other energy production systems, but it is of limited utility in pharmaceutical analysis. In this article, a molybdenum disulfide composite was prepared, and the electro-activity of MoS₂ toward the oxidation of omeprazole (OMZ) was investigated. The molybdenum disulfide content of the prepared material was quantified by thermal gravimetric analysis (TGA), its crystallinity revealed by X-ray diffraction (XRD), and its topographic features were probed by scanning electron microscopy (SEM). Glassy carbon electrode was modified by MoS₂, and the electrochemical activity of the modified electrode toward omeprazole oxidation was investigated in a phosphate buffer solution (pH 7.00) using differential pulse voltammetry (DPV). The well-resolved anodic peak at ca. 0.85 V vs Ag/AgCl was reported at the modified and bare glassy carbon electrodes. The impact of the modification with MoS₂ was noticed as a 2.3-fold enhancement of the OMZ oxidation current. Under the applied experimental conditions and utilising the modified electrode, a linear response was obtained in the range of 15.8–500. μM with a limit of detection equal to 4.74 μM and a correlation coefficient of 0.989. The modified electrode was also employed to detect omeprazole in its commercial pharmaceutical formulations. Percent recovery values of 84.0 to 100.% were reported.

Keywords: Omeprazole, Voltammetry, Surface Analysis, Catalysis, Molybdenum disulfide.

Introduction

Omeprazole, a substituted imidazole, is abbreviated as OMZ and nomenclated as 6-methoxy-2-((4-methoxy-3,5-dimethylpyridin-2-yl) methylsulfonyl)-1H-benzo[d]imidazole. A look at the structure of omeprazole, Figure 1, reveals that it has a chiral sulfur centre^[1]. In one of its resonance structures, where the π electrons shared between the sulfur and the adjacent

oxygen are located on the oxygen, OMZ could be looked at as a molecule where the central sulfur is connected to four different moieties; the benzimidazole, the pyridine ring, the negatively charged oxygen atom, and the lone pair located on the sulfur atom^[2]. Therefore, omeprazole exists as a racemic mixture, the R-enantiomer, already known as omeprazole, and the S-enantiomer, referred to as esomeprazole. Both

*Corresponding Authors: M. F. Khanfar
E. S. M. Abu-Nameh

Email: mohammad.khanfar@giu.edu.jo
abunameh@bau.edu.jo

forms are of similar pharmaceutical significance^[3].

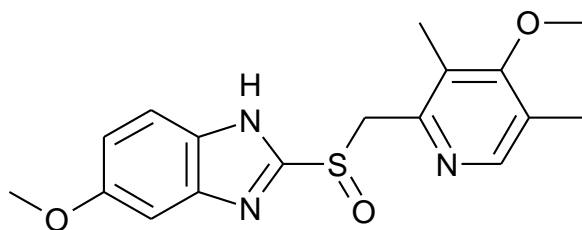


Figure 1. Chemical structure of Omeprazole.

Omeprazole is a proton pump inhibitor (PPI); it acts as an anti-ulcer and anti-gastric to counteract the backflow of secretions from the stomach into the oesophagus (gastroesophageal disease) that suppresses stomach acid output, both at rest and when activated. OMZ blocks the so-called proton pump of the parietal cell, which is thought to be the last step in the acid secretory pathway^[4–6].

Omeprazole has been quantified by three key instrumental methods, photometry, chromatography and electrochemistry^[7]. The PPI was analyzed as either an individual analyte, a combination of two or more species or as an unmetabolized species that co-exists with its metabolites^[8–13]. Omeprazole has been detected in simple matrices such as standard OMZ solutions or as an ingredient in complicated systems such as commercial pharmaceutical formulations and human fluids.

There is a commonality between the chromatographic and the photometric detection of omeprazole since most of the performed chromatographic OMZ separation is coupled with photometric detection^[14–17]. The photodetector, in-line with the chromatographic setup, is tuned at the omeprazole absorption maxima under the applied experimental conditions. Signals of the eluted OMZ could be easily correlated to omeprazole concentration. In the absence of significant interfering agents, electrochemical detection could be used in pharmaceutical analysis. Potential step, as well as potential sweep techniques, have been widely used for the detection of a wide range of active pharmaceutical ingredients such as sulfamethoxazole, tadalafil, trimethoprim and hydrochlorothiazide, among others^[18–21]. Also, omeprazole voltammetric detection has been widely conducted with the utilization of electrodes of different compositions^[22–25].

Voltammetric methods provide easy, comfortable, sensitive and straightforward protocols for analysis. In this work, omeprazole was determined voltammetrically at a glassy carbon electrode modified with molybdenum disulfide, a chalcogenide that is usually used in energy systems such as fuel cells and supercapacitors^[26–29]. The modified electrode was used in this work to detect OMZ as a standard and a blended ingredient in commercial pharmaceutical formulations. To the best of our knowledge, MoS₂ has not been employed for the determination of omeprazole.

Materials and Methods

Omeprazole was obtained from Hikma Pharmaceuticals, Amman, Jordan, and was used as received. Potassium dihydrogen phosphate, dipotassium hydrogen phosphate, Nafion (5 wt% sulfonic acid polymer in lower aliphatic alcohols and water, contains 15–20% water) and molybdenum disulfide were all provided by Sigma-Aldrich, Milwaukee, WI, USA. Sodium hydroxide, ethanol and potassium chloride were purchased from VWR Chemicals International, Radnor, PA, USA. The used carbon black was Vulcan XC72R, a kind gift from Cabot Corp., Alpharetta, GA, USA.

De-ionized water was obtained from aquamax 372 Youngin water purification system, YOUNG IN Chromass Co., Ltd., Republic of Korea. All the electrochemical measurements were performed in a pH 7.00 phosphate buffer (0.010 M) solution. KCl (0.10 M) was used as the supporting electrolyte and to adjust the ionic strength, while NaOH (1.0 M) was used to adjust the pH value of the working solution. The pH was probed by Orion Star A211 Benchtop pH Meter, Thermo Fisher Scientific Inc., Waltham, MA, USA.

The content of omeprazole in three different commercial formulations was analyzed in this work. One of the formulations was manufactured locally (capsules), while the other two were imported from Switzerland (capsules) and Germany (tablets). Solid phase extraction was performed using the vacuum manifold and the accompanying pump provided by J.P. Selecta, Abrera, Barcelona, Spain. C₁₈-SPE cartridges were used in the recovery studies and were supplied by MACHEREY-NAGEL GmbH & Co. KG, Düren, Germany.

Catalyst Preparation and Characterization

MoS₂ was physically mixed with the Vulcan XC72R carbon at a 25:75 mass percentage, respectively. The total mass of the powder was about 500. mg. The mixture was added to 100. mL phosphate buffer (pH 7.00, 0.010 M) and then refluxed for two hours. The powder was left to cool down and finally collected by simple filtration. The powder mixture was characterized by Scanning Electron Microscopy (SEM), X-ray Powder Diffraction (XRD) and Thermal Gravimetric Analysis (TGA). The catalyst was SEM imaged using a Vega III Tescan microscope, Breno, Czech Republic. Diffraction measurements were performed using a Phaser 2D benchtop diffractometer, Bruker, Karlsruhe, Germany, with Cu-K_α line as a source. A TG 209 F1 Libra thermogravimetric analyzer, NETZSCH GmbH, Selb, Germany, was used to determine the content of molybdenum sulfide in the catalyst powder.

Electrode Modification and Electrochemical Measurements

10 mg of the catalyst powder was mixed with 300 μL Nafion and 700 μL ethanol. The combination was sonicated for 30. minutes to secure the formation of a homogeneous phase, commonly known as black ink. To fully cover the surface area of the working electrode, 3 μL of the prepared ink was applied atop a previously polished glassy carbon electrode, which was then left to air dry.

Cyclic Voltammetric (CV), Electrochemical Impedance Spectroscopy (EIS) and Differential Pulse Voltammetry (DPV) have been performed in phosphate buffer solutions (pH 7.00, 0.010 M) in a three-compartment glass cell. Ag/AgCl and platinum were used as the reference and the counter electrodes, respectively. The measurements were performed in neutral pH 7.00 phosphate buffer solutions since omeprazole undergoes acid degradation at pH values lower than 4.00^[7]. Model PGSTAT 204 potentiostat, Metrohm Autolab BV, Utrecht, the Netherlands, with 302 FRA module, was used for the electrochemical measurements. Cyclic voltammetric measurements were performed by scanning the potential of the carbon electrodes between -0.10 to 1.3 V vs Ag/AgCl. The impedance measurements were performed in the 100 MHz–10 mHz range, while the differential voltammetric measurements were performed by

scanning the potential of the working electrodes between 0 and 1.2 V vs Ag/AgCl. The following parameters were used for the voltammetric measurements: potential step 0.005 V, modulation amplitude 0.025 V, modulation time 0.05 s, interval time 0.5 s, at a scan rate of 0.010071 V/s.

Recovery Studies

To obtain percentage recovery of the active ingredient in the analyzed commercial formulations using the modified electrode, one tablet or the powder content of one capsule of each of the provided drugs was weighed and powdered with mortar and pestle. The powder was then accurately transferred to a 100-mL volumetric flask and diluted to the mark with the prepared buffer solutions. The solutions were then sonicated for 10 minutes, filtered using the solid phase extraction setup, and then a fraction of the filtrate was pipetted and used for the recovery evaluation. %Recovery was then estimated based on the following equation:

$$\%Recovery = \frac{S_{x+s} - S_x}{S_s} \times 100\%$$

S_x and S_s are the oxidation peak current values for the sample and the standard pharmaceutical solutions, respectively, and S_{x+s} is the oxidation peak current for mixtures of equal volumes of the standard and the sample solutions. The recovery measurements were performed in sets of three replicates.

Results and Discussion

The presence of molybdenum disulfide, as one of the two ingredients of the catalyst, was verified by SEM imaging of the prepared catalyst, as shown in Figure 2. Figure 2 presents the screened catalyst at three different magnification scales, 500, 3000, and 5000. In Figure 2a, the molybdenum disulfide appears as small islands atop the carbon surface. Features of the disulfide become more distinguishable as the magnification is increased. Figure 2b shows how the disulfide exists in the form of agglomerates. Sheets or flakes of the disulfide are shown in Figure 2c^[30,31]. Hence, SEM confirms the presence of the disulfide as a component of the binary catalyst besides the carbon powder. For comparative purposes, the molybdenum disulfide-free powder was SEM screened, as shown in Figure 2d. The flake-like features are

absent from the figure that shows carbon powder particles scattered randomly over the imaged surface. The bright spots shown in Figure 2d could be attributed to carbon aggregates

accumulated at levels higher than the average level of most of the imaged carbon particles.

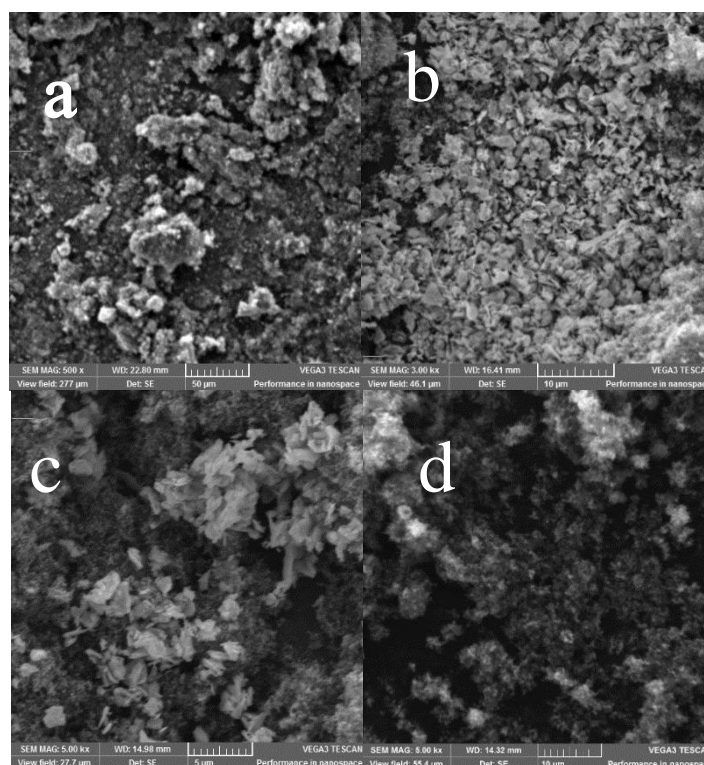


Figure 2. SEM images of MoS₂ modified carbon, (a) 500×, (b) 3000×, (c) 5000× and (d) molybdenum sulfide-free carbon surface.

The XRD pattern of molybdenum disulfide is shown in Figure 3. It shows the common planes of crystalline molybdenum disulfide^[32,33]. Although the correlation of the catalyst activity to its crystallinity is beyond the scope of the current research, XRD successfully proves that the disulfide does exist as a component in the catalyst in a crystalline form. On the other hand, the peaks assigned for MoS₂ are absent from the corresponding diffractogram of the molybdenum disulfide-free carbon powder (Figure 3).

As mentioned in the experimental section, MoS₂ was mixed with the carbon powder at 25:75-mass percentage, respectively. Thermal gravimetric analysis (Figure 4) points to the presence of 26.1 mass percent, left after the removal of the carbon content of the analyzed catalyst at temperatures higher than 500 °C. The insignificant mismatch between the nominal and the experimental mass contents could be attributed to a loss in carbon powder during the different steps of the catalyst preparation, such as weighing and filtration.

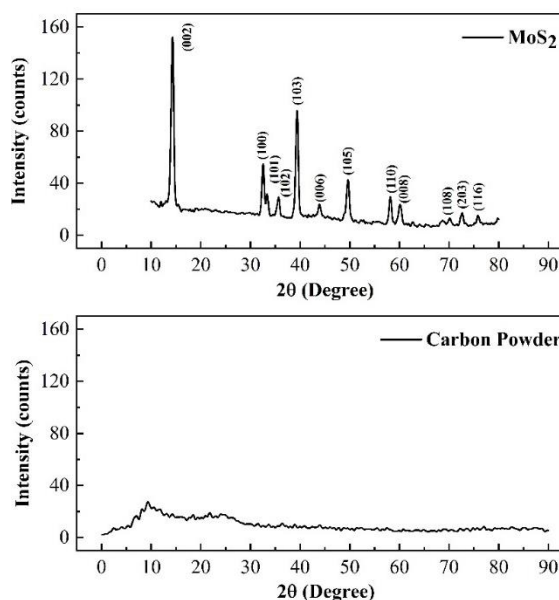


Figure 3. XRD patterns of MoS₂/carbon catalyst and carbon powder.

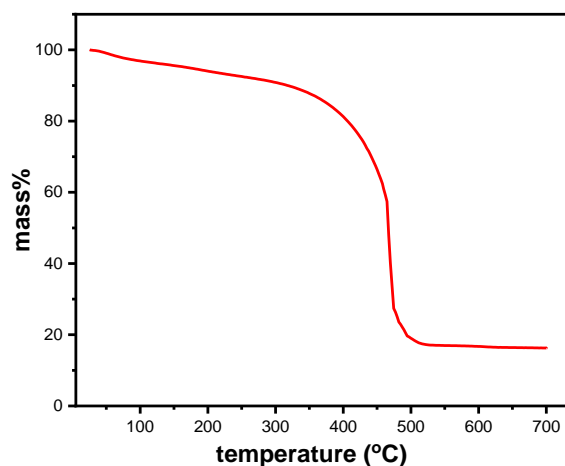


Figure 4. Thermogram of the MoS₂/carbon catalyst

The conductivity of the bare and the MoS₂-modified electrodes could be revealed by electrochemical impedance spectroscopy. Figure 5 shows the Nyquist plots for the mentioned electrodes in the omeprazole-free buffer solution (pH 7.00). The figure demonstrates the significant difference in impedance between the modified and the bare surfaces over a wide range of frequencies, especially in the high-frequency range, where the impedance of the bare surface is significantly higher than that of the MoS₂-modified surface. The observed difference could be directly attributed to the higher conductivity of the modified surface over the bare electrode^[34,35].

The voltammetric behaviour of the bare and the modified electrodes in the buffer solution (pH 7.00) is presented in Figure 6. There is no specific conclusion to withdraw from the figure since only water oxidation is observed at potentials higher than 1.00 V. It is, however, obvious

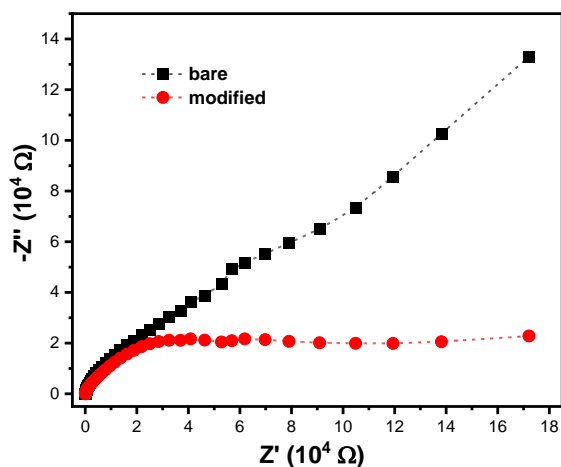


Figure 5. Nyquist plots of the bare and the MoS₂-modified glassy carbon electrodes.

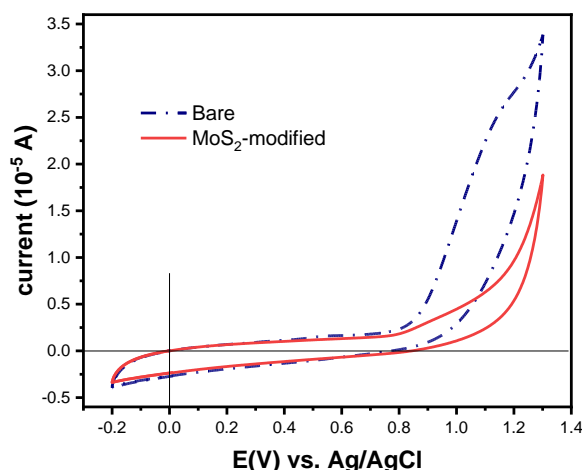


Figure 6. Cyclic voltammograms of the bare and the modified electrodes in 0.10 M PBS (pH 7.00); Scan rate = 25 mV/s.

that the bare electrode demonstrates a relatively higher activity toward water oxidation, which is not in the scope of the conducted work.

To explore the efficiency of the MoS₂-modified electrode toward the oxidation of omeprazole, its electrochemical behaviour has been investigated. Cyclic voltammetry was used to reveal any electrochemical activity of the modified electrode in 0.500 mM omeprazole in the aqueous buffer solution (pH 7.00). Figure 7 shows that, at the modified electrode, the oxidation starts at potentials higher than 0.80 V, which can be attributed to the oxidation of omeprazole.

Assignment of the omeprazole oxidation potential could not be easily withdrawn from cyclic voltammetric experiments. This is because

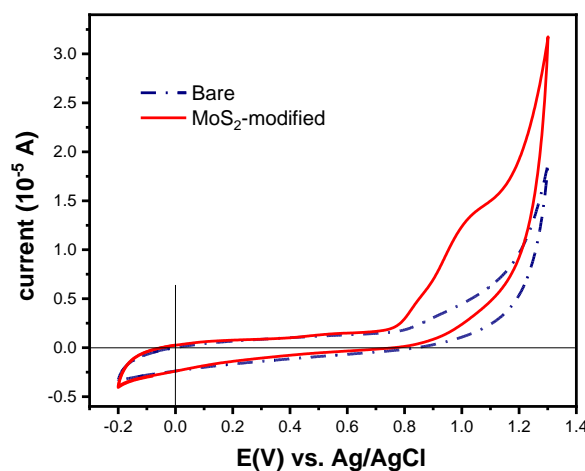


Figure 7. Cyclic voltammograms of the bare and the modified electrodes in 0.500 mM omeprazole in 0.10 M PBS (pH 7.00); Scan rate = 25 mV/s.

cyclic voltammetry belongs to a group of electrochemical sweep methods where the current generated in the potential sweep is a combination of two components, the Faradaic current and the capacitive current^[36,37]. The capacitive current is related to the charging-discharging nature of the double layer between the working electrode and the adjacent aqueous phase; therefore, it is not relevant to the electrochemical interfacial process taking place at the electrode surface. The desired information resides in the Faradaic current, which is directly related to the electrolysis of the target analyte, and, consequently, to the analyte concentration since the Faradaic current is correlated to the amount oxidized or reduced.

To discriminate between the capacitive and the Faradaic current components, differential pulse voltammetry (DPV) was utilized in this work. Figure 8 showed an enhancement in the oxidation current when the MoS₂-modified electrode was used for omeprazole oxidation.

The electrochemical oxidation process is demonstrated in Figure 9: Omeprazole is oxidized in a $-1e^-/-1H^+$ oxidation step into its 5-hydroxy counterpart, a well-known and characterized metabolite of omeprazole^[38-40]. The reported catalytic activity could be

attributed to the nature of the modifier, molybdenum disulfide. Although not conductive as metals, molybdenum disulfide is well-known for its high surface area, a feature it has in common with graphite sheets. In addition, it exhibits strong adsorption affinity toward electro-active analytes such as omeprazole, and as a result, it facilitates their electrolysis at the working electrode surface^[41-43].

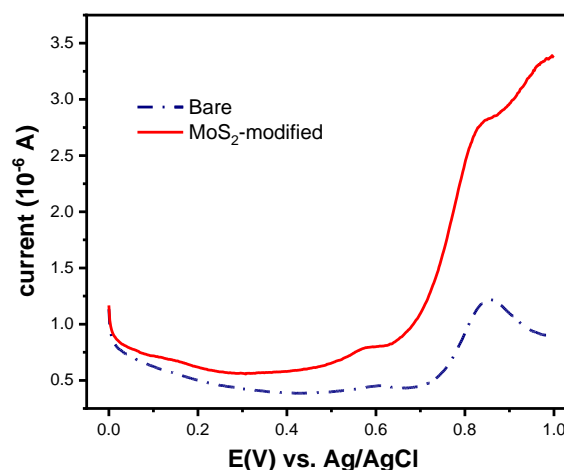


Figure 8. Differential pulse voltammograms of the bare and the modified electrodes in 0.100 mM omeprazole in PBS (pH 7.00); Scan rate = 5.00 mVs⁻¹

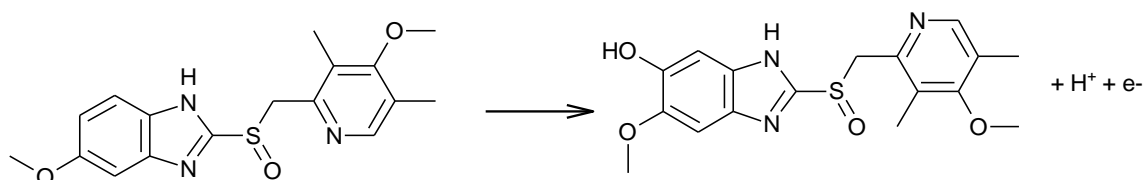


Figure 9. Electro-oxidation of omeprazole.

Estimation of figures of merit

The reported enhancement in the oxidation current shown in Figure 8 was utilized to estimate the key figures of merit related to the application of the modified electrode for omeprazole quantification. A calibration curve was established from the relationship between the concentrations of standard omeprazole solutions and the corresponding oxidation peak current values at the MoS₂-modified surface (Figure 10). A slope (m) of 0.0199 A/M was estimated, while the corresponding standard deviation (σ) was found to be equal to 3.16×10^{-8} . The corresponding limits of detection (LOD) and quantitation (LOQ) were obtained from the standard deviation of the blank and the slope of the calibration curve (Figure 10) as follows:

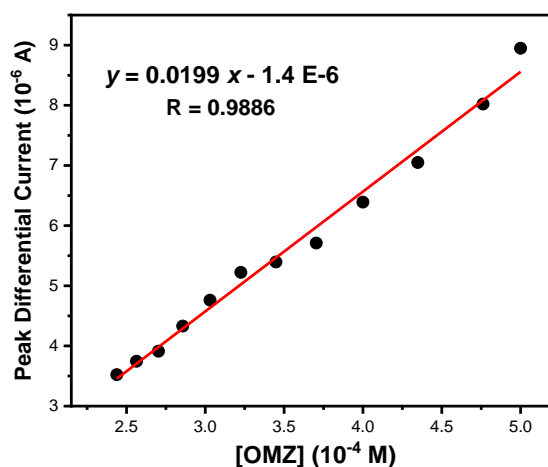


Figure 10. Differential pulse voltammograms of the modified electrode in 0.100 mM OMZ in PBS (pH 7.00) at different concentrations; scan rate = 5.00 mVs⁻¹.

$$\text{LOD} = 3 \sigma/m = 4.74 \times 10^{-6} \text{ M}$$

$$\text{LOQ} = 10 \sigma/m = 1.58 \times 10^{-5} \text{ M}$$

Therefore, based on these estimated values, the method could be employed for the detection of omeprazole in any concentration falling in the range between $1.58 \times 10^{-5} \text{ M}$ and $5.00 \times 10^{-4} \text{ M}$. A straightforward comparison of the performance of the MoS₂-modified electrode to other

electrodes applied for omeprazole detection (Table 1), points to the need to improve the efficiency of the electrode studied in this work. From Table 1, it can be concluded that the MoS₂-modified electrode exhibits a relatively higher limit of detection and a shorter dynamic range. These issues need to be investigated in the upcoming related studies.

Table 1. Comparison of the reported parameters with their corresponding published values.

Working Electrode	Sample	LOD	Dynamic Range	Reference
Fe ₃ O ₄ -MWCNT	Tablets, Capsules, Waste Water, Urine, Serum	15 nM	0.05-9.0 μM	40
Zinc Ferrite-Graphene	Plasma, Formulations	0.015 μM	0.030-100 μM	44
Poly alizarin	Commercial Capsules	0.715 μM	0.4-1 mM	45
PANI-MWCNT	Commercial Formulations	47.2 μg/ml	100-600 μg/ml	46
MoS ₂ -modified GCE	Commercial Formulations	4.74 μM	15.8 -500 μM	This work

Regardless of the reported shortcomings, the molybdenum disulfide electrode provided acceptable recovery percentages when used to estimate the recovery of three omeprazole-containing formulations. Table 2 lists the screened drugs and the reported recovery values. All obtained percentages were within the accepted limits for recovery studies, between 80.0 and 120.%. The ability of the modified electrode to recognize and oxidize omeprazole in the presence of co-existing ingredients is an added value that proves the necessity to improve the performance of the presented method. For example, the voltammograms related to estimating the percent recovery of the Swiss drug are shown in Figure 11.

Table 2. Recovery estimation for three commercial omeprazole brands.

Brand	Form	Recovery %
Jordanian	Capsules	100
Swiss	Capsules	84
German	Tablets	95

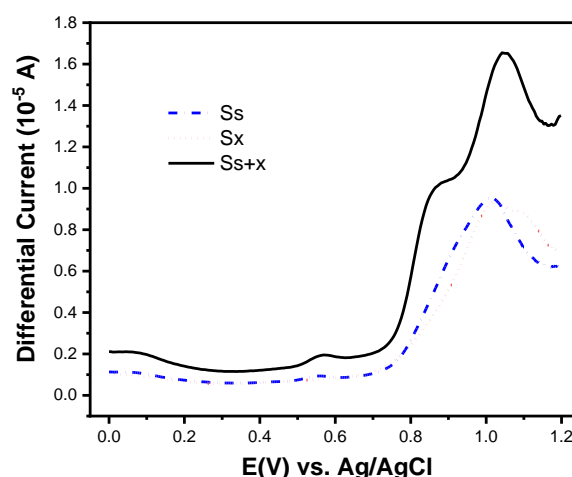


Figure 11. Recovery estimation of a Swiss pharmaceutical containing omeprazole. S_s, S_x, and S_{s+x} are the signals obtained for the standard, drug and mixture.

Conclusion

In this work, glassy carbon electrodes were utilized for the electrochemical determination of omeprazole. The electrode was modified by MoS₂. The resulting carbon-MoS₂ mixture was characterized by XRD, SEM, EIS and TGA, which verified the presence of the molybdenum disulfide catalyst, its content and conductivity. The modified electrode had proven a significantly improved performance over its bare

counterpart, especially when a potential step method, namely differential pulse voltammetry, was used. The reported activity was attributed to the affinity of the disulfide layer to adsorb electroactive species, such as omeprazole.

Although more active than its bare analogue, the modified electrode was found to be of lower catalytic performance when compared to other

modified electrodes reported in the literature. The shortcomings could be summarized as showing a rather high limit of detection and a short dynamic range. Improvement of performance of the utilized catalyst may be achieved by insertion of conductive materials, or by manipulation of the thickness of the modifier, factors that will be considered in the future.

References

- [1] Abelö, A.; Andersson, T. B.; Antonsson, M.; Naudot, A. K.; Skånberg, I.; Weidolf, L., *Drug Metab. Dispos.*, **2000**, 28, 966–972.
- [2] Caner, H.; Cheeseman, J. R.; Agranat, I., *Chirality*, **2006**, 18, 10–16.
- [3] Unge, S.V.; Langer, V.; Sjölin, L., *Tetrahedron Asymmetry*, **1997**, 8, 1967–1970.
- [4] Olbe, L.; Carlsson, E.; Lindberg, P. A., *Nat. Rev. Drug Discov.*, **2003**, 2, 132–139.
- [5] Blume H.; Donath F.; Warnke A.; Schug, B. S., *Drug Saf.*, **2006**, 29, 769–784.
- [6] Horn, J., *Clin. Ther.*, **2000**, 22, 266–280.
- [7] Espinosa Bosch, M.; Ruiz Sánchez, A. J.; Sánchez Rojas, F.; Bosch Ojeda, C., *J. Pharm. Biomed. Anal.*, **2007**, 44, 831–844.
- [8] Jia, H.; Li, W.; Zhao, K., *J. Chromatogr. B*, **2006**, 837, 112–115.
- [9] Rahman, A.; Haque, M. R.; Sultan, M. Z.; Rahman, M. M.; Rashid, M. A., *Dhaka Univ. J. Pharm. Sci.*, **2018**, 16, 221–233.
- [10] Ekpe, A.; Jacobsen, T., *Drug. Dev. Ind. Pharm.*, **1999**, 25, 1057–1065.
- [11] Di Giacinto, J. L.; Olsen K. M.; Bergman, K, L.; Hoie, E. B., *Ann. Pharmacother.*, **2000**, 34, 600–605.
- [12] Jensen B.P.; Smith, C.; Wilson, I. D.; Weidolf, L., *Rapid Commun. Mass Spectrom.*, **2004**, 18, 181–183.
- [13] González, H. M.; Romero, E. M.; de J. Chavez, T.; Peregrina A. A.; Quezada, V.; Hoyo-Vadillo, C., *J Chromatogr. B Analyt. Technol. Biomed. Life Sci.*, **2002**, 780, 459–465.
- [14] Borges, K. B.; Durán-Patrón, R.; Sánchez, A. J. M.; Pupo, M. T.; Bonato, P. S.; Collado, I. G., *J. Braz. Chem. Soc.*, **2011**, 22, 1140–1149.
- [15] Ahmad, L.; Iqbal, Z.; Nazir, S.; Shah, Y.; Khan, A.; Khan, M. I.; Nasir, F.; Khan, A., *J. Liq. Chromatogr. Relat. Technol.*, **2011**, 34, 1488–1501.
- [16] Linden, R.; Ziulkoski, A. L.; Wingert, M.; Tonello, P.; Souto, A. A., *J. Braz. Chem. Soc.*, **2007**, 18, 733–740.
- [17] DellaGreca, M.; Iesce, M. R.; Previtera, L.; Rubino, M.; Temussi, F.; Brigante, M., *Chemosphere*, **2006**, 63, 1087–1093.
- [18] Khanfar, M. F.; Absi, N.; Abu-Nameh, E.; Saket, M.; Khorma, N.; Daoud, R.; Alnuman, N., *Int. J. Electrochem. Sci.*, **2019**, 14, 3265–3280.
- [19] Khanfar, M. F.; Abu-Nameh, E. ; Afaneh, A. ; Saket, M. ; Ahmad, A. ; Faraj, W. ; Khalil, M. ; Khotaba, H. ; Bujog, M., *Bulg. Chem. Commun.*, **2019**, 51, 305–311.
- [20] Khanfar, M. F. ; Abu-Nameh, E.; Saket, M. M.; Al Khateeb, L. T.; , Al Ahmad, A.; Asaad, Z.; Salem, Z.; Alnuman, Nasim., *Int. J. Electrochem. Sci.*, **2020**, 15, 1771–1787.
- [21] Abu-Nameh, E.; Al Absi, N.; Al-Wahish, M. A.; Hodali, H. A. ; Khanfar, M. F., *Int. J. Electrochem. Sci.*, **2020**, 15, 6396–6404.

- [22] Pinzauti, S.; Gratteri, P.; Furlanetto, S.; Mura, P.; Dreassi, E.; Phan-Tan-Luu, R., *J. Pharm. Biomed. Anal.*, **1996**, *14*, 881–889.
- [23] Radi, A., *J. Pharm. Biomed. Anal.*, **2003**, *31*, 1007–1012.
- [24] Ghandour, M.A.; Hassan, A.; Ali, H.M., *J. Anal. Chem.*, **2015**, *70*, 392–397.
- [25] Stefano, J. S.; Tormin, T. F.; da Silva, J. P.; Richter, E. M.; Munoz, R. A. A., *Microchem. J.*, **2017**, *133*, 398–403.
- [26] Xinrong, G.; Wang, Y.; Wu, F.-Y.; Ni, Y.; Kokot, S., *Analyst*, **2015**, *140*, 1119–1126.
- [27] Benavente, E.; Santa Ana, M. A.; Mendizábal, F.; González, G., *Coord. Chem. Rev.*, **2002**, *224*, 87–109.
- [28] Sun, D.-Y.; Lin, B.-Z.; Xu, B.-H.; He, L.-W.; Ding, C.; Chen, Y.-L., *J. Porous Mater.*, **2008**, *15*, 245–251.
- [29] Li, H.; Ahn, S. H.; Park, S.; Cai, L.; Zhao, J.; He, J.; Zhou, M.; Park, J.; Zheng, X., *Appl. Phys. Lett.*, **2016**, *109*, 133103 (5 pages).
- [30] Rajalakshmi, S.; Dhanalakshmi, S.; Chen, S.-M.; Chen, T.-W.; Selvam, V.; Ramaraj, S. K.; Weng, W.-H.; Leung, W.-H., *Int. J. Electrochem. Sci.*, **2017**, *12*, 9288–9300.
- [31] Liu, L.; Zhengquan, L.; Huang, P.; Wu, Z.; Shuyun, J., *RSC Adv.*, **2016**, *6*, 113315–113321.
- [32] Zhou, K.; Jiang, S.; Bao, C.; Song, L.; Wang, B.; Tang, G.; Hu, Y.; Gui, Z., *RSC Adv.*, **2012**, *2*, 11695–11703.
- [33] Du, G.; Guo, Z.; Wang, S.; Zeng, R.; Chen, Z.; Liu, H.-K., *Chem. Commun.*, **2010**, *46*, 1106–1108.
- [34] Wang, Y.; Mamat, X.; Yongtao, L.; Hu, X.; Wang, P.; Dong, Y.; Hu, G., *Electroanalysis*, **2019**, *31*, 1390–1400.
- [35] Huang, H.; Zhang, J.; Cheng, M.; Liu, K.; Wang, X., *Microchim. Acta*, **2017**, *184*, 1–6.
- [36] Bond, A. M.; Oldham, B. K.; Zoski, G. C., *Anal. Chim. Acta*, **1989**, *216*, 177–230.
- [37] Batchelor-McAuley, C.; Kätelhön, E.; Barnes, E.; Compton, R.; Laborda, E.; Molina, A., *ChemistryOpen*, **2015**, *4*, 224–260.
- [38] Jorge, S. M. A.; Pontinha, A. D. R.; Oliveira-Brett, A. M., *Electroanalysis*, **2010**, *22*, 625–631.
- [39] Kalate Bojdi, M.; Behbahani, M.; Mashhadizadeh, M. H.; Bagheri, A.; Hosseiny D.; Saied, S.; Farahani, A., *Mat. Sci. Eng. C*, **2015**, *48*, 213–219.
- [40] Deng, K.; Liu, X.; Li, C.; Hou, Z.; Huang, H., *Sens. Actuators B Chem.*, **2017**, *253*, 1–9.
- [41] Mani, V.; Govindasamy, M.; Chen, S.M.; Subramani, B.; Sathiyam, A.; Merlin, J.P., *Int. J. Electrochem. Sci.*, **2017**, *12*, 258–267.
- [42] Maachou, L.; Qi, K.; Petit, E.; Qin, Z.; Zhang, Y.; Cot, D.; Flaud, V.; Reibel, C.; El-Maghrabi, H.; Li, L.; Miele, P.; Kaplan, D.; Chhowalla, M.; Onofrio, N.; Voiry, D., *J. Mater. Chem. A*, **2020**, *8*, 25053–25060.
- [43] Abbasi, P.; Asadi, M.; Liu, C.; Sharifi-Asl, A.; S. S.; Sayahpour, B.; Behranginia, A.; Zapol, P.; Shahbazian-Yassar, R.; Curtiss, L.; Salehi-Khojin, A., *ACS Nano*, **2017**, *11*, 453–460.
- [44] Afkhami, A.; Bahiraei, A.; Madrakian T., *J. Colloid Interface Sci.*, **2017**, *495*, 1–8.
- [45] Mahanthesha, K. R.; Swamy, K.; Pai, K.V., *Anal. Bioanal. Electrochem.*, **2014**, *6*, 234–244.
- [46] Karolia, P.; Tiwari, D.; Jain, R., *Ionics*, **2015**, *21*, 2355–2362.